An Evaluation of Strength Performance of the Edge Connections between Cross-laminated Timber Panels Reinforced with Glass Fiber-reinforced Plastic

Yo-Jin Song, In-Hwan Lee, and Soon-Il Hong *

The strength performance of edge connections between the cross-laminated timber (CLT) panels, as currently applied to CLT construction, was compared to that of connections reinforced with glass fiber-reinforced plastic (GFRP) by means of a tensile-type shearing test. In this study, the reinforced half-lapped connection is intended to prevent CLT from coming apart due to failure of self-tapping screws (STS) by bonding GFRP sheets to connections between CLT panels. The end-distance and edge-distance of this reinforced half-lapped connection were designed to equal 5D (where D is the fastener diameter) and 4D, respectively, which is shorter than the 6D recommended by European Technical Approval (ETA). Nevertheless, the yield strength was increased by 7%, and the stiffness by 92%, compared to the non-reinforced half-lapped connection. In addition, the internal spline connections using GFRP-reinforced plywood were 57 and 36% higher than the connection made up of LVB or plywood, respectively, and the energy dissipation percentages were 400 and 76%, respectively. These results indicate that the reinforcement effect of the connection by the GFRP was very significant. On the other hand, the half-lapped connection of the larch CLT improved the strength performance as the end-distance increased, and the end-distance had a greater effect on the strength performance than the edge-distance.

Keywords: Cross-laminated timber; CLT edge connection; Self-tapping screw; Half-lapped; Spline; Shear test; Shear test; Glass fiber-reinforced plastic

*Contact information: College of Forest & Environmental Sciences, Kangwon National University, Chun-Cheon 200-701, Republic of Korea; *Corresponding author: hongsi@kangwon.ac.kr*

INTRODUCTION

Cross-laminated timber (CLT) panels contain longitudinally laminated laminae that are cross-laminated one by one. As they can be fabricated in an infinite size in theory, no edge connection between the panels is required. Because an extremely large CLT cannot be shipped, appropriate-sized CLTs are field-connected and expanded to the required size (Nakashima *et al*. 2012; Oh *et al*. 2017). In the CLT structural system, more connections between the panels result in increased construction cost and reduced strength against the horizontal load. As these connections are the main source of ductility and energy dissipation capability, however, the CLT buildings with connections demonstrate excellent seismic performance. Therefore, the behavior of the connection largely determines the overall performance of the structure, making it a key factor in maintaining the structural integrity, strength, and stability of the building (Ceccotti *et al*. 2006; Dujic and Zarnic 2006; Follesa *et al*. 2010).

Several studies have been carried out on the half-lapped and spline connections, which are the most representative of the CLT panel-edge connection, due mainly to their simple process, minimal waste of wood, and easy construction in the field. Sadeghi *et al*. (2015) reported that the half-lapped and single-surface spline connections have low strength relative to bending moments. Given the economics and ease of construction, however, they still have a sufficient potential to improve the design of the connection (Sadeghi *et al*. 2015). Gavric *et al*. (2012) reported that the half-lapped connections have higher stiffness than the single-surface spline connections. Brittle failure due to a plug shear was observed, however, in the half-lap of some specimens (Gavric *et al*. 2012). Follesa *et al*. (2010) studied the strength performance of the half-lapped, internal spline, and single-surface spline connections, as well as their ease of operation and further cost for the workforce. The study results showed that the actual strength of the connections was 1.5 times higher than the value calculated according to EN 1995-1-1 (2004), the criterion for solid wood and glulam, *etc*., due to the cross-lamination effect. In addition, the stiffness and difference were significant, as the formula according to EN 1995-1-1 (2004) is calculated without considering the thickness of the layer and the metal type of the fastener used. In terms of cost, nails are cheaper than screws, and the half-lapped connections are the least expensive (Follesa *et al*. 2010). Sullivan (2017) showed in a shear test for the half-lapped and single-surface spline connections that the connection strength increased in proportion to the diameter of the self-tapping screw (STS), but higher ductility was measured when using STSs with an 8 mm diameter rather than STSs with a 10 mm diameter.

On the other hand, cracks occurring along the end-distance or edge-distance were frequently found in the neck joint using metal joints such as STS, dowel, and bolt (Oh *et al*. 2017; Ottenhaus *et al.* 2018). Therefore, methods to increase the end-distance and edge-distance of the joints or to suppress the failure rate by reinforcing the joint were applied to suppress potential failure. The reinforcement of members and joints using fiber-reinforced plastic (FRP) in wood structure has been shown to be effective when applied to solid wood or glulam, prompting the authors to conclude that it would improve strength performance if it is applied to side joints between CLT panels (Kim *et al* 2013; Raftery and Harte 2011; Song *et al* 2017).

In this study, the performance of the lateral connections between CLT panels using glass fiber-reinforced plastic (GFRP) was evaluated for the reinforcement of the typical lateral connections between CLT panels.

EXPERIMENTAL

Material

Cross-laminated timber

In this study, a five-layer CLT (thickness: 130 mm) was fabricated using larch laminae (*Larix kaempferi* Carr.), which were classified by their respective modulus of elasticity using the visual stress grading method (KSF 3021 2016). The longitudinal layer consisted of grade 2 or higher-grade laminae, and the transverse layer consisted of grade 3 or lower-grade laminae. Phenol-resorcinol formaldehyde adhesive (PRF) was used as a bond between laminae, and the adhesive spread rate was set at 400 g/m2 (single spread) while the pressing pressure was set at 0.7 MPa.

Spline

For the spline, larch plywood and radiate pine LVB (*Pinus radiate* D. Don.), which satisfy the KS F 3101 criteria, were used, and a reinforced plywood in which a 6-mm-thick GFRP was laminated onto an 18-mm-thick plywood was also used. The GFRP consisted of a fabric-type glass cloth that was inserted in a glass fiber plastic sheet to suppress the potential cleavages generated in a general sheet along the direction of the glass fiber. Polyvinyl acetate resin (PVAc) was used as a bond between GFRP and plywood (Park *et al*. 2009). The splines were 24 mm thick, and their mean density were 553.4 kg/m^3 (plywood), 530.0 kg/m^3 (LVB), and 901.1 kg/m^3 (reinforced plywood).

Fig. 1. Shape of reinforced plywood with GFRP plate

Fastener

The STS made by Wurth (Künzelsau, Germany) was used for the CLT edge connection. The diameter of the STS was less than 1/10 of the thickness of the CLT, and STSs with different diameters and lengths were used depending on the connection type (DIBT 2013). The shape and size of the fastener are shown in Table 1 and Fig. 2. According to Sheikhtabaghi (2015), the tensile strength and shear strength increased by 5% when a washer was inserted in the half-lapped connection in the case of the STS measuring 8 mm in diameter, while in the single-surface spline connection, the tensile strength increased by 41% and the shear strength increased by 61%. In this study, there was no need to insert a separate washer on the screw head, but an STS with a wider screw head was used.

Table 1. Dimensions and Strength of Self-Tapping Screws (CCMC 2013)

Fastener Type	Thread Diameter (*D*)	Thread Length (*lg*)	Head Diameter (*dh*)	Fastener Length (*l*)	Bending Yield Strength	Screw Shear Strength
					MPa	*MPa*
Self-tapping Screw	8 mm	80 mm	22 mm	120 mm	1015	641
	6 mm	70 mm	14 mm	120 mm	969	578
	6 mm	42 mm	14 mm	70 mm		

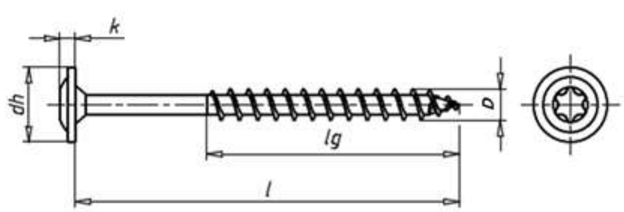

Fig. 2. Schematic diagram of the self-tapping screw (Würth 2016)

Methods

Fabrication of a tension-type shear test specimen

The European Technical Approval (ETA) specifies that the minimum end distance and minimum edge distance of the CLT should be 6D (D: Thread diameter of fastener) (DIBT 2013). In this study, the test specimens were fabricated according to the end distance, edge distance, and reinforcement of the half-lapped connections based on the 6D standard (Table 2). In Series-1, the end distance was made to 5D, 6D, and 7D, respectively, with the edge distance fixed to 6D, while in Series-2, the end distance was made to 4D, 5D, and 6D, respectively, with the edge distance fixed to 7D (Fig. 3). Series 3 was reinforced by applying GFRP to the top side of the half-lap after applying stringent design specifications: end distance to 5D and edge distance to 4D (Fig. 6). The half-lapped test specimens were connected together by STS measuring 8 mm (d) × 120 (l).

Table 2. Test Program Summary

Connection Type	End Distance	Edge Distance	Spline Type	Screw (*mm*)	Test Series	No. of Specimens
Half-lapped	5D	6D	-	8 × 120	Series-1-5D-6D	6
	6D	6D		8 × 120	Series-1-6D-6D	6
	7D	6D		8 × 120	Series-1-7D-6D	6
	7D	4D		8 × 120	Series-2-7D-4D	6
	7D	5D		8 × 120	Series-2-7D -5D	6
	7D	6D		8 × 120	Series-2-7D -6D	6
	5D	4D		8 × 120	Series-3-reinforced	9
Internal Spline	7D	5D	LVB	6 × 120	Series-4-LVB	5
	7D	5D	Plywood	6 × 120	Series-5-plywood	5
	7D	5D	Reinforced Plywood	6 × 120	Series-6-R-plywood	6
Double-Spline	7D	4D	Reinforced Plywood	6 × 70	Series-7-R-plywood	4

The spline connections were designed to have the same end distance of 7D and the same groove height of 24 mm. The test specimen of the internal spline connections was fabricated by inserting LVB (Series-4), plywood (Series-5), and reinforced plywood (Series-6), and then fastening them using two STSs (6 mm (d) × 120 mm (l)) so that the edge distance would measure up to 5D (Fig. 4). The test specimen of the double-spline specimens was fastened together using reinforced plywood (Series-7) and four STSs (6mm (d) × 120mm (l)) so that the edge distance would measure up to 4D and the spacing perpendicular to a plane parallel to the grain would measure up to 2D (Fig. 5).

The STS head was nailed so it would not protrude out of the CLT surface, by drilling a hole with an area and a thickness corresponding to those of the STS head when inserting the STS into the all test specimens to prevent the wood from being damaged by the STS head during the test.

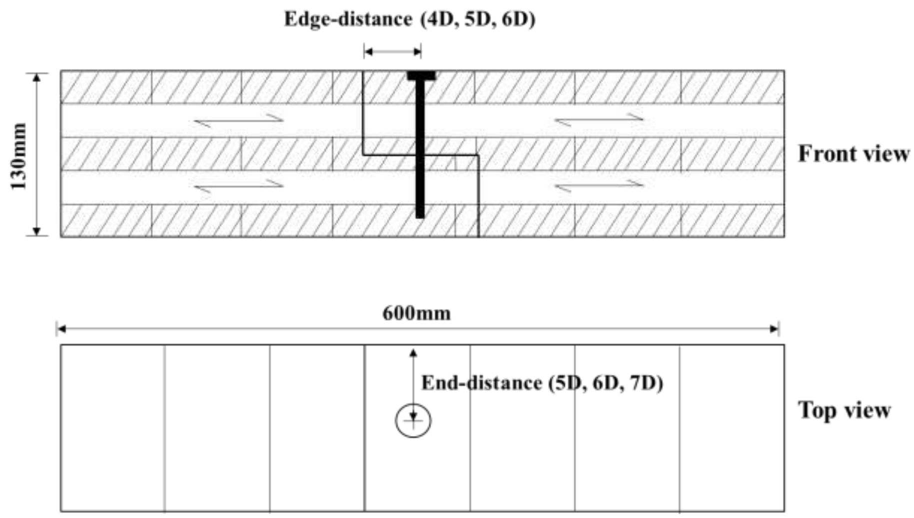

Fig. 3. Schematic diagrams of the half-lapped connection specimen

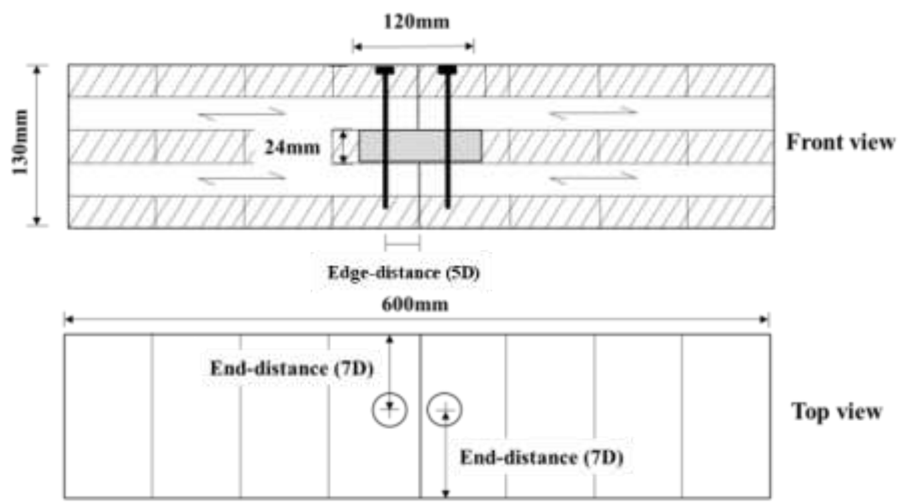

Fig. 4. Schematic diagrams of the internal spline connection specimen

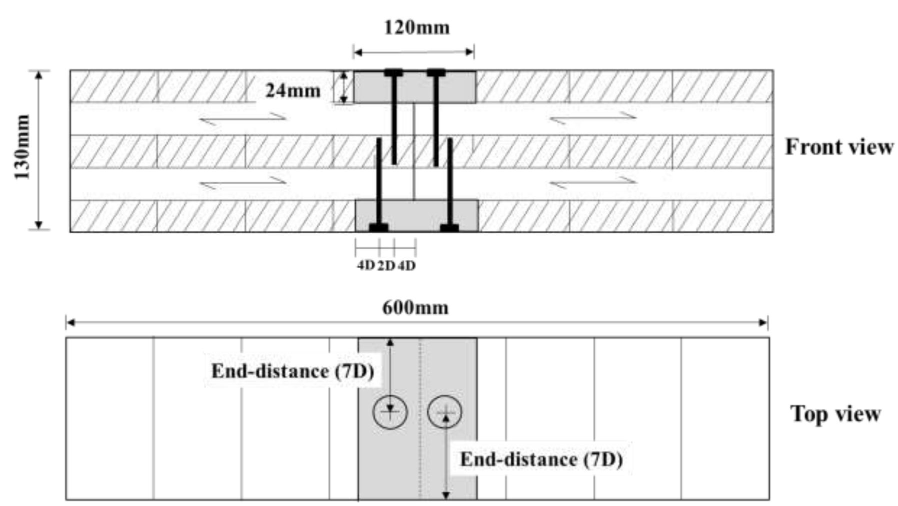

Fig. 5. Schematic diagrams of the double-spline connection specimen

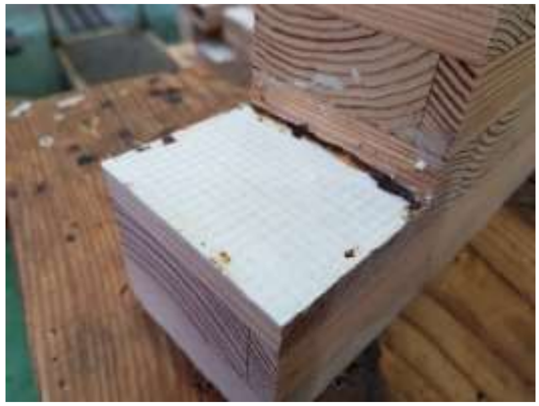

Fig. 6. Half-lapped connection reinforced with GFRP

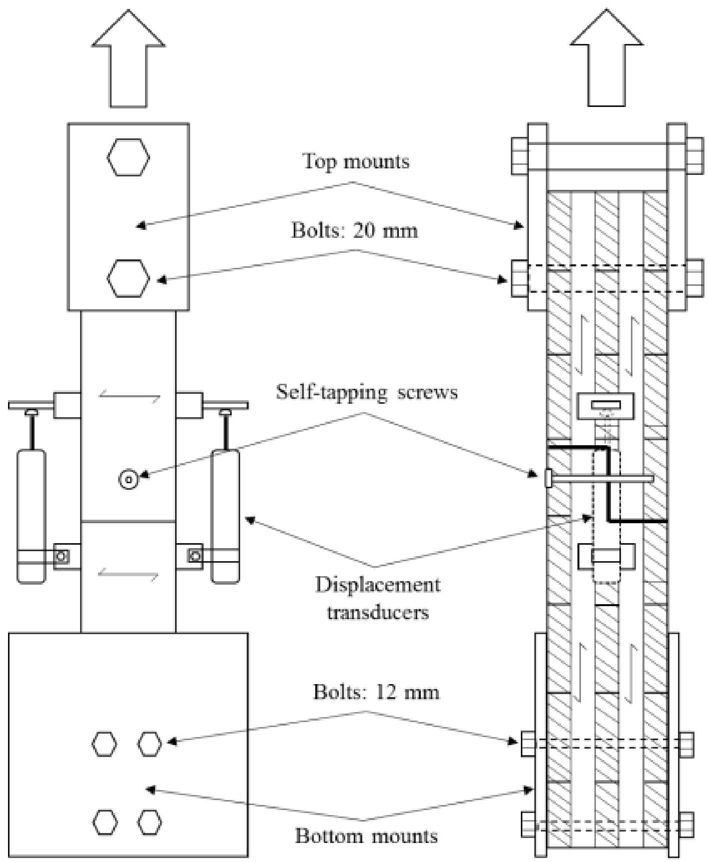

Fig. 7. Schematic diagram of the tension test on the edge connections between the CLT panels

Tension-type shear test

A vertical load testing machine with a maximum capacity of 30 tons was used for the tension-type shear test. As shown in Fig. 7, two displacement transducers (CDP-50) with a maximum capacity of 50 mm were installed on the left and right sides of the CLT connection test specimen by fastening them using two 20 mm diameter bolts at the top mounts of the specimen and four 12 mm diameter bolts at the bottom mounts. In this study, only the monotonic test was carried out, and the loading rate was set to 5 mm/min according to ASTM D5652-07 (2007) so that the specimen would fail in between 5 and 20 min.

RESULTS AND DISCUSSION

Load and Deformation

Figures 8 and 9 are representative load-deformation curves of the half-lapped and spline connections, drawn using the mean strain values of the two displacement transducers and the load values of the load cell. Table 3 shows the maximum load and failure load of the test specimens. The failure load was assumed to be 80% when the failure of the test specimen was not clearly visible on the load-deformation curve or during the test.

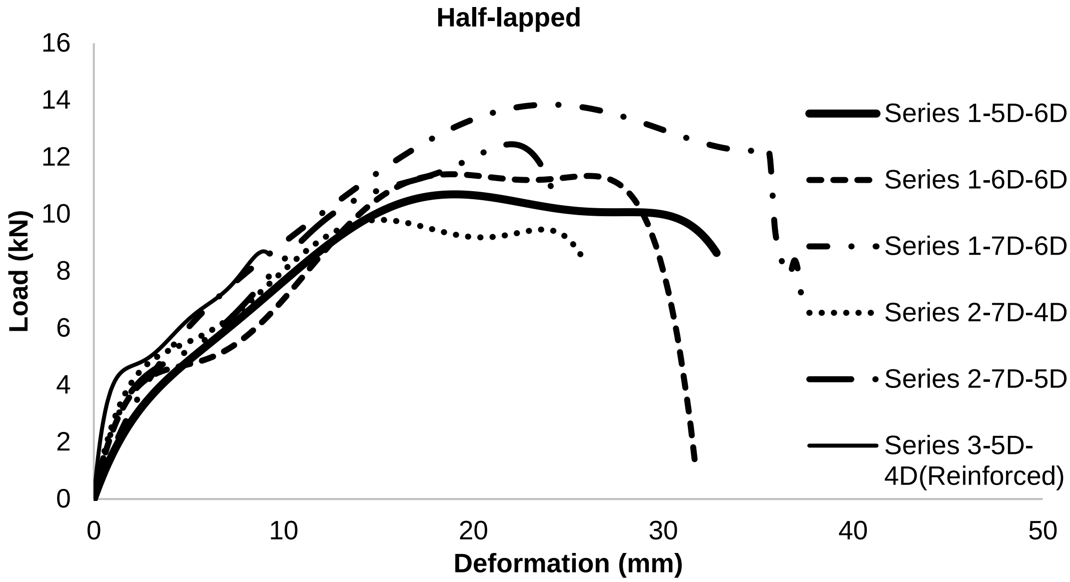

Fig. 8. Typical load-deformation curves of the half-lapped connection for the tension test

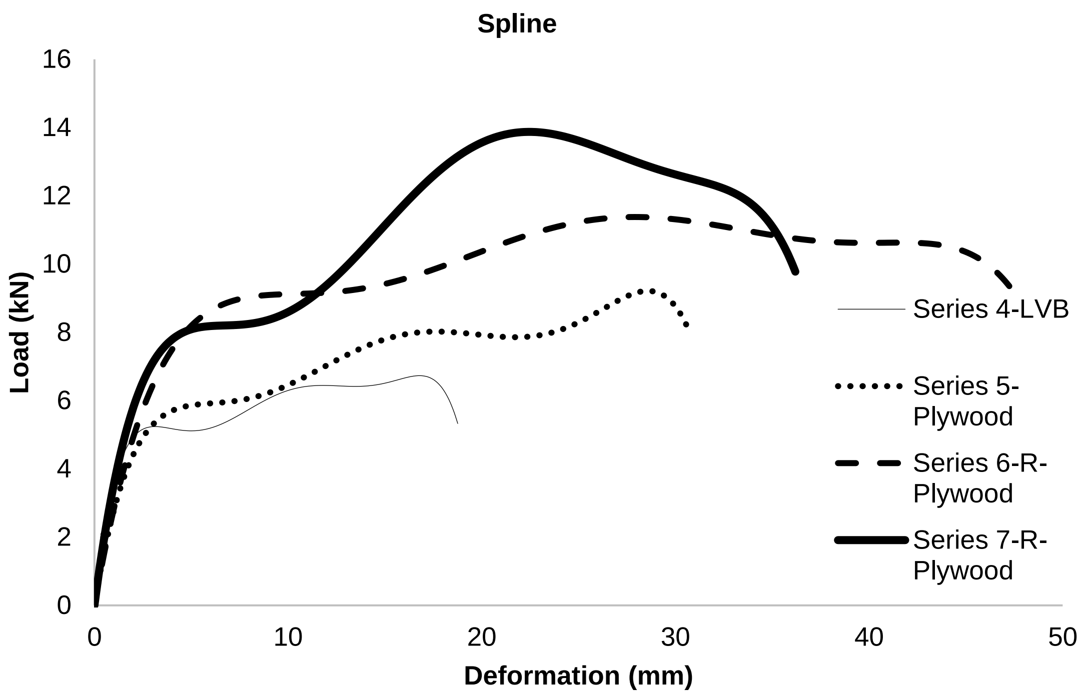

Fig. 9. Typical load-deformation curves of the spline connection for the tension test

In the case of Series-3-Reinforced, in which the half-lap was reinforced with GFRP, failure occurred at a low deformation section, the reason being that the maximum load and the failure load were the lowest among the half-lapped connections. The coefficient of variation was also measured to be the greatest. These results were due to the differences in failure mode, depending on whether reinforcement was present, which is explained in "Failure mode." In the case of the internal spline connection, the maximum load was determined to be 49% higher than that of the LVB when connected with plywood, whereas that of the reinforced plywood was determined to be 28% higher than that of plywood. The load did not decrease rapidly after the maximum load was reached in the case of the reinforced plywood, unlike the other splines. Kim's previous study on the bolt connection of the glass fiber-reinforced glulam showed that the reinforcement with sheet-type GFRP with the same direction as the grain direction of the wood increased the maximum load by 14% compared with the untreated glulam, while the reinforcement with a fabric-type glass cloth increased the maximum load by 51% (Kim and Hong 2016). Given that the GFRP tested in this study was a type in which glass cloth was inserted in the sheet, it was believed to have a high load value because reinforced plywood does not fail easily due to STS. The maximum load of the double-spline connection was determined to be 14% higher than that of the internal spline connection. It was maintained that the two types of connections showed differences in their respective maximum loads because more STS were used for the double-spline connections though they were both double shear connections.

Meanwhile, as the end distance increased, the maximum load and failure load tended to increase as well. In particular, when the end distance increased from 6D to 7D, the maximum load and failure load increased by 23% and 36%, respectively. As the edge distance increased from 4D to 5D, the maximum load and failure load increased by 31% and 20%, respectively, but no significant increase was observed between 5D and 6D.

Table 3. Load and Deformation Properties of the Edge Connections between the CLT Panels

Connection Type	Test Series	F_{max} (kN)	Δ_{max} (mm)	$F_{failure}$ (kN)	$\Delta_{failure}$ (mm)
Half-lapped	Series-1-5D-6D	10.69 (6.6)*	18.08 (13.1)	8.95 (8.6)	23.16 (20.0)
	Series-1-6D-6D	11.45 (15.8)	20.89 (28.3)	9.42 (13.6)	29.71 (10.5)
	Series-1-7D-6D	14.16 (8.1)	24.12 (23.3)	12.79 (10.4)	29.68 (25.5)
	Series-2-7D-4D	10.33 (16.1)	18.34 (28.4)	9.35 (19.8)	22.95 (23.1)
	Series-2-7D-5D	13.50 (10.6)	22.54 (18.7)	11.20 (14.6)	29.89 (18.9)
	Series-2-7D-6D	14.16 (8.1)	24.12 (23.3)	12.79 (10.4)	29.68 (25.5)
	Series-3-Reinforced	9.10 (27.1)	11.80 (8.0)	8.65 (23.3)	12.67 (8.0)
Internal Spline	Series-4-LVB	6.08 (12.5)	14.62 (13.7)	4.91 (8.9)	20.73 (8.5)
	Series-5-Plywood	9.03 (4.6)	31.86 (11.9)	8.11 (6.1)	34.40 (13.0)
	Series-6-R-Plywood	11.57 (3.9)	32.01 (28.2)	9.32 (2.9)	43.53 (10.3)
Double-spline	Series-7-R-Plywood	13.45 (11.9)	26.01 (28.9)	11.45 (16.8)	32.83 (24.6)
( )* = Coefficient of variation (%)					

Yield Load and Initial Stiffness

The structure must remain elastic under gravity loads. Seismic design, however, permits plastic deformation of ductile structures. It is therefore very important to know the yield point at which plastic begins to deform (Muñoz *et al*. 2008). The yield of timber connections, however, is difficult to define if there is no clear and present change in the stiffness (Sheikhtabaghi 2015). Thus, several methods of identifying the yield points on the load-deformation curve have been studied. In this study, the 5% offset method, one of the commonly used methods, in which the actual yield point can be determined on the load-deformation curve, was employed according to ASTM D5652-07 (2007).

The maximum load of Series-3-Reinforced was lower than that of the other half-lapped connection specimens, but the yield load and initial stiffness were determined to be 3.60 kN and 4.99 kN/mm, respectively. This means that GFRPs in the shear section suppressed embedment failure of the wood caused by STS decisively by 7% and 92%, respectively, as compared to the average yield load and average initial stiffness of the other half-lapped connections. The half-lapped connections that were not reinforced showed a low coefficient of variation due to high strength of the fasteners and the embedding failure of the wood. In the case of Series-3-Reinforced GFRP, however, it inhibited the embedment failure of wood by fasteners, but failure occurred due to the stresses concentrated in the woody area where reinforcement starts. It is believed in this case that the difference in the directions of age rings as well as the gap between earlywood and latewood in woody may have pushed up the coefficient of variation of the test specimens.

In the internal spline connection, the yield load difference between Series-4-LVB and Series-5-Plywood was not significant, but the yield load of Series-6-R-Plywood was determined to be 32% higher than the average yield load of the two other Series. On the other hand, the initial stiffness was slightly different depending on the spline type, although the difference was not significant. The yield load between Series-7-R-Plywood and Series-6-R-Plywood did not show any significant difference.

The yield load increased with increasing end distance, and the yield load increase rate was the largest when the end distance increased from 6D to 7D. The yield load increased the largest when the edge distance increased from 4D to 5D, at which point the coefficient of variation was very low. On the other hand, the initial stiffness was not affected by the increase in the end distance and edge distance.

Table 4. Yield Load and Initial Stiffness of the Edge Connections between the CLT Panels

Connection Type	Test Series	F_{yield} (*kN*)	Δ_{yield} (*mm*)	*K* (*kN/mm*)
Half-lapped	Series-1-5D-6D	3.13 (24.0)*	1.70 (27.6)	2.79 (47.7)
	Series-1-6D-6D	3.20 (13.1)	1.80 (14.4)	2.11 (12.8)
	Series-1-7D-6D	3.50 (9.4)	1.92 (21.8)	2.48 (27.8)
	Series-2-7D-4D	3.18 (36.8)	1.55 (23.9)	3.22 (57.1)
	Series-2-7D-5D	3.60 (11.7)	1.85 (18.4)	2.50 (14.0)
	Series-2-7D-6D	3.50 (9.4)	1.92 (21.8)	2.48 (27.8)
	Series-3-Reinforced	3.60 (15.8)	1.15 (20.0)	4.99 (27.5)
Internal Spline	Series-4-LVB	3.46 (16.8)	1.60 (11.3)	2.63 (29.3)
	Series-5-Plywood	4.00 (7.5)	2.08 (10.6)	2.12 (19.3)
	Series-6-R-Plywood	5.42 (5.2)	2.50 (8.4)	2.36 (12.7)
Double-spline	Series-7-R-Plywood	5.33 (8.8)	1.98 (18.2)	3.20 (22.8)
( ) = Coefficient of variation (%)*				

Ductility and Energy Dissipation

Strength and stiffness are also important for seismic performance, but ductility is crucial for determining how much plastic deformation a building can undergo without a significant loss of strength. A single CLT without an edge connection demonstrates high stiffness but lacks ductility because it is a rigid body. Therefore, it is important to design the module in such a way that it would have a proper ductility through a lateral connection of panels. The ductility ratio of the connection was calculated using Δ_{max} on the load-deformation curve, as shown in Eq. 1. Smith *et al.* (2006) classified the ductility ratios that were calculated according to the proposed grades.

$$D_{max} = \Delta_{max} / \Delta_{yield} \tag{1}$$

The ductility ratios of the half-lapped, internal spline, and double-spline connections were measured to be 6 or more, thereby confirming their excellent ductility. In the case of the half-lapped connection, there was no significant correlation between the increases of the end distance and edge distance and their ductility ratios. In Series-3-Reinforced, where high yield loads were measured, the small Δ_{max} and Δ_{yield} were measured due to early failure, and the ductility ratio was calculated to be the lowest. On the other hand, there was almost no difference in the ductility ratio between Series-6-R-Plywood of the internal spline and Series-7-R-Plywood of the double-spline.

Table 5. Ductility Ratio and Energy Dissipation of the Edge Connections between the CLT Panels

Connection Type	Test Series	D_{max}	Ductility Classification	$W_{failure}$ ($kN \cdot mm$)
Half-lapped	Series-1-5D-6D	11.35 (25.0)*	High	168.23 (30.9)
	Series-1-6D-6D	11.46 (16.2)	High	257.40 (22.5)
	Series-1-7D-6D	12.74 (17.7)	High	308.89 (33.1)
	Series-2-7D-4D	11.88 (21.0)	High	171.40 (31.9)
	Series-2-7D-5D	12.22 (11.0)	High	300.38 (28.7)
	Series-2-7D-6D	11.88 (21.9)	High	308.89 (33.1)
	Series-3-Reinforced	9.71 (31.7)	High	91.71 (80.4)
Internal Spline	Series-4-LVB	9.28 (20.9)	High	104.30 (6.9)
	Series-5-Plywood	15.33 (6.3)	High	237.95 (12.5)
	Series-6-R-Plywood	12.77 (26.0)	High	419.22 (14.9)
Double-spline	Series-7-R-Plywood	12.97 (10.6)	High	336.80 (31.7)

( )* = Coefficient of variation (%)

The energy dissipation of the connection is a concept describing the ability to absorb and disperse the external force, and there is a method of calculating it until 30 mm deformation and until the failure deformation, as proposed by EN 12512 (DIN 2002). The energy dissipation up to the failure deformation was measured in this study because some of the test specimens experienced failure deformation before the deformation reached 30 mm. The energy dissipation up to the failure deformation was calculated by measuring the internal area from the test start point to the failure deformation point ($\Delta failure$) on the load-deformation curve.

In the case of the half-lapped connection, the energy dissipation capacity tended to increase as the end distance increased, and the edge distance increased greatly from 4D to 5D. The energy dissipation capacity of Series-3-Reinforced was very low due to the early failure of the woody area where reinforcement began. Among the internal spline connections, Series 6-R-Plywood showed 4 times higher energy dissipation capacity than Series-4-LVB and 1.8 times higher energy dissipation than Series-5-Plywood, while Series-7-R-Plywood also demonstrated an excellent energy dissipation capacity. These results show that reinforced plywood has a higher load and a wider deformation zone after passing the yield load on the spline connection.

Failure mode

Figure 10 shows the typical failure mode in the tension-type shear test of the CLT edge connection. The half-lapped connections reduce the volume of the middle lamina by half-lapping. Therefore, regardless of the end distance and edge distance, the middle laminae of most of the test specimens in this study were destroyed in the end distance direction when they reached the failure load. The failure was especially prominent in the middle lamina of CLT, where the STS head was inserted in a high proportion (Mode A). This failure mode was caused by the STS head acting as a washer. The STS on the side of the head did not significantly deform due to the shear force, and no breakage due to the acupressure occurred in the woody part. On the other hand, a wood fracture occurred due to a local pressure, which was triggered by the pulling out of the thread portion of the opposite side of the head. Additionally, net tension failure occurred due to the STS in some test specimens, in which a quarter sawn lamina was placed on the transverse layer.

Failure of the un-reinforced half-lapped connections and reinforced half-lapped connections (Series-3-Reinfored) were both affected by end-distance. In the case of the un-reinforced test specimen, it cannot be expected to have a high strength when applied to a real CLT panel due to the failure of the fastener to the adjacent fastener. On the other hand, in the case of the reinforced tucked test specimen, it failed because of the stresses concentrated on the part of the wood where the reinforcement starts, rather than due to the embedment failure caused by the fastener (Mode B). Therefore, a high tensile strength can be expected here because there is a series of wood sections where there volumes have been halved.

In the case of Series-3-Reinforced, the reinforced GFRP prevented the failure of the woody part due to the bearing failure on the STS, but failure occurred at a point where the relatively weak volume began to decrease by half (the area where reinforcement began) (Mode B). Like the unreinforced half-lapped test specimens, the head of the STS affected the failure of the connection.

In the internal spline connection, a bearing failure occurred in the spline by the STS in Series-4-LVB and Series-5-Plywood (Mode C). On the contrary, the STS head was sucked into the woody part of the CLT due to the high strength of the spline in Series-6-R-Plywood, thereby tearing out the CLT instead (Mode D). In Series-7-R-Plywood, a bearing failure occurred in the process of the STS being pulled out of the CLT (Mode E).

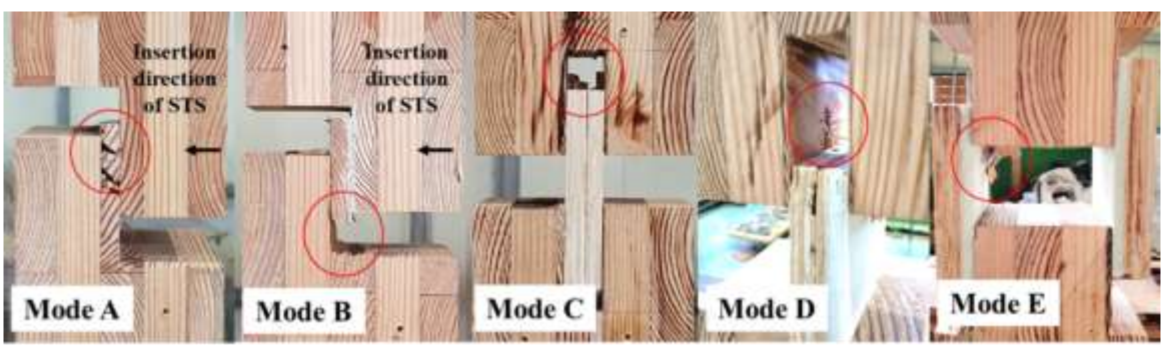

Fig. 10. Failure modes of the edge connections between the CLT panels

CONCLUSIONS

1. In this study, the shear strength performance of the cross-laminated timber (CLT) half-lapped connection and spline connection using glass fiber-reinforce plastic (GFRP) was evaluated. The yield strength of half-lapped connections reinforced by GFRP was higher than that of typical half-lapped connections, although the end-distance and edge-

distance were designed to be shorter than the reference. It was also observed that GFRP suppressed the indentation failure of wood by fasteners decisively.

2. The connections using GFRP-reinforced plywood in spline connections showed the best strength performance and 1.7 times higher yield strength than the half-lapped connections that were designed in accordance with the standards (Series-1-6D-6D). In case of double-spline, on the other hand, it was confirmed that efficiency difference was not significant although the two reinforced plywood were used, because of the difference in strength performance between internal spline connections.

3. Meanwhile, as the end-distance and edge-distance of the half-lapped connection increases, the strength increases as well. In the case of larch CLT, in particular, the yield strength increased from 6D to 7D based on the end-distance standard, while the yield strength of edge-distance was kept quite high even when the end distance was decreased from 6D to 5D.

REFERENCES CITED

ASTM D5652-07 (2007). "Standard test methods for bolted connections in wood and wood-based products," ASTM International, West Conshohocken, USA. DOI: 10.1520/d5652

Canadian Construction Material Center (CCMC) (2013). *Evaluation Report CCMC 13677-R SWG ASSY and VG plus and SWG ASSY 3.0 Self-tapping Wood Screws,* Ottawa, Canada. (www.my-ti-con.com/resources/ccmc-code-approval-13677-r/download).

Ceccotti, A., Follesa, M., Lauriola, M. P., and Sandhaas, C. (2006). "SOFIE project-test results on the lateral load resistance of cross-laminated wooden panels," in: *1st European Conference on Earthquake Engineering and Seismology (a joint event of the 13th ECEE & 30th General Assembly of the ESC,* Geneva, Switzerland, pp. 1-10.

EN 1995-1-1 (2004). "Eurocode 5 - Design of timber structures - Part 1-1: General common rules and rules for buildings," European Committee for Standardization, Brussels, Belgium.

DIBT (2013). "Würth self-tapping screws," *European Technical Approval ETA-11/0190,* IfB, Berlin, Germany. (http://www.wuerth.it/download/products/certificazioni_tasselli/eta_11_0190_eng_2013.pdf).

DIN EN 12512-02 (2002). "Timber structures, test methods, cyclic testing of joints made with mechanical fasteners," Beuth Verlag, Berlin, Germany. DOI:10.3403/02536208 u

Dujic, B., and Zarnic, R. (2006). "Study of lateral resistance of massive X-Lam wooden wall system subjected to horizontal loads," in: *International Workshop on Earthquake Engineering on Timber Structures,* Comibra, Portugal, pp. 97-104.

Follesa, M., Brunetti, M., Cornacchini, R., and Grasso, S. (2010). "Mechanical in-plane joints between cross laminated timber panels," in: *11th World Conference on Timber Engineering,* Trentino, Italy, pp. 1-6, (http://www.dedalegno.com/imgPUBBLICAZIONI/Articoli_scientifici/2010_wcte2010_Mechanical%20in%20plane.pdf).

Gavric, I., Fragiacomo, M., and Ceccotti, A. (2012). "Strength and deformation characteristics of typical X-Lam connections," in: *12th World Conference on Timber Engineering,* Auckland, New Zealand, pp. 146-155, (http://support.sbcindustry.com/Archive/2012/july/Paper_092.pdf?PHPSESSID=ju29kfh90oviu5o371pv47cgf3).

Kim, K. H., and Hong, S. I. (2016). "Estimate of bolt connection strength of reinforced glulam using glass fiber," *Journal of The Korean Wood Science and Technology* 44(1), 67-74. DOI: 10.5658/WOOD.2016.44.1.67

Kim, K. H., Song, Y. J., and Hong, S. I. (2013). "Shear strength of reinforced glulam-bolt connection by glass fiber combination," *Journal of The Korean Wood Science Technology* 41(1), 51-57. DOI: 10.5658/WOOD.2013.41.1.51

KSF 3021 (2016). "Structural glued laminated timber," Korean Standards Association, Seoul.

Muñoz, W., Salenikovich, A., Mohammad, M., and Quenneville, P. (2008). "Determination of yield point and ductility of timber assemblies: In search for a harmonized approach," in: *Proceedings of the 10th* WCTE, Miyazaki, Japan, pp. 1064-1071, (https://pdfs.semanticscholar.org/c9e2/4eb4009d006bfcc961d8daa53fccd07b7b6e.pdf).

Nakashima, S., Kitamori, A., Mori, T., and Komatsu, K. (2012). "Evaluation of tensile performance of drift pin joint of cross laminated timber with steel inserted plate," in: *World Conference on Timber Engineering 2012*, Auckland, New Zealand, pp. 417-424, (http://support.sbcindustry.com/Archive/2012/july/Paper_050.pdf?PHPSESSID=s13roe79b9bf8iusgahtvboh36).

Oh, J. K., Kim, G. C., Kim, K. M., Lee, J. J., and Hong, J. P. (2017). "End distance of single-shear screw connection in cross laminated timber," *Journal of The Korean Wood Science Technology* 45(6), 746-752. DOI: 10.5658/WOOD.2017.45.6.746

Ottenhaus, L-M., Li, M., Smith, T., and Quenneville, P. (2018). "Overstrength of dowelled CLT connections under monotonic and cyclic loading," *Bulletin of Earthquake Engineering* 16(2), 753–773. DOI: 10.1007/s10518-017-0221-8

Park, J. C., Shin, Y. J., and Hong, S. I. (2009). "Bonding performance of glulam reinforced with glass fiber-reinforced plastics," *Journal of The Korean Wood Science and Technology* 37(4), 357-363. DOI: 10.5658/WOOD.2009.37.4.357

Raftery, G., and Harte, A. (2011). "Low-grade glued laminated timber reinforced with FRP plate," *Composite: Part B* 42(4), 724-735. DOI: 10.1016/j.compositesb.2011.01.029

Sadeghi, M., Ballerini, M., Smith, I., and Pedrotti, E. (2015). "Bending properties of connections in cross laminated timber," in: *International Association for Bridge and Structural Engineering (IABSE) Conference 2015 May 13-15*, Nara, Japan, pp. 1-8. DOI: 10.2749/222137815815775402

Sheikhtabaghi, M. S. (2015). *Continuity Connection for Cross Laminated Timber (CLT) Floor Diaphragms*, Master's Thesis, University of New Brunswick, Fredericton, Canada, (https://unbscholar.lib.unb.ca/islandora/object/unbscholar%3A6923/datastream/PDF/view).

Smith, I., Asiz, A., Snow, M., and Chui, Y. H. (2006). "Possible Canadian / ISO Approach for deriving design values from test data," in: *International Council for Research and Innovation in Building and Construction Working Commission W-18 (Timber Structures)*, Florence, Italy, pp. 85-86, (http://www.cib-w18.com/sites/all/themes/traeinfo/reviews/2_Materials.pdf).

Song, Y. J., Suh, J. S., Park, S. B., Hong, S. I. (2017). "Strength performance evaluation of moment resistance for cylindrical-LVL column using GFRP reinforced wooden pin," *Wood Research* 62(3), 417-426, (www.woodresearch.sk/wr/201703/07.pd f).

Sullivan, K. (2017). *Behavior of Cross-laminated Timber Diaphragm Panel-to-panel Connections with Self-tapping Screws*, Master's Thesis, Oregon State University, Corvallis, USA, (http://hdl.handle.net/1957/60149).

Würth (2016) *Assy®-Die Schraube für das Holz-und Bauhandwerk*, Germany, (https://ww w.wuerth.de/ web/media/downloads/pdf/ipa/ASSY_2016.pdf).

Article submitted: October 24, 2018; Peer review completed: January 13, 2019; Revised version received: July 30, 2019; Accepted: July 31, 2019; Published: August 7, 2019.
DOI: 10.15376/biores.14.4.7719-7733